Journal of Physics:
Conference Series

PAPER • **OPEN ACCESS**

Solid-state Hydrogen storage: influence of storage capacity in physisorption

To cite this article: Costantino Barbieri *et al* 2024 *J. Phys.: Conf. Ser.* **2893** 012057

Journal of Physics: Conference Series **2893** (2024) 012057 doi:10.1088/1742-6596/2893/1/012057

Solid-state Hydrogen storage: influence of storage capacity in physisorption

Costantino Barbieri[1], **Vito Ceglie**[1], **Michele Stefanizzi**[1], **Marco Torresi**[1]

[1] Polytechnic University of Bari, Department of Mechanics, Mathematics & Management, via Orabona 4, 70125 Bari, Italy

E-mail: costantino.barbieri@poliba.it

Abstract.

Hydrogen storage in solid-state is a promising alternative to conventional technologies to overcome some of their limitations, particularly in terms of the amount of hydrogen stored per unit volume. For instance, liquid hydrogen (stored at 1 bar and 20 K) is characterized by a 70.8 kg/m^3 volumetric density, but a great amount of energy is required for liquefaction (about 12.5 kWh/kg); whereas, hydrogen stored as compressed gas (350 - 700 bar) at ambient temperature reaches a density ranging from 24.5 to 41.4 kg/m^3, however the compression work is significant, and the high storage pressure determines safety issues. Regarding solid-state hydrogen storage, chemisorption is a solution, where hydrogen is stored at moderate pressure and temperature, reaching a volumetric density of 80-110 kg/m^3, but between hydrogen and metal hydrides chemical bonds born, which require a significant amount of energy to be break them; moreover, the time required for absorption and desorption is very low. In the context of solid-state storage, carbon materials can be an interesting solution due to their low cost, and their ability to store hydrogen reversibly within a porous structure through physisorption mechanisms, under supercritical conditions. This study numerically investigates the effect of the variation of the tank capacity on the charging, dormancy, and discharging processes. Two similar axi-symmetric geometries are considered by doubling the tank volume from V_1 = 2.5 L to V_2 = 5 L. The physisorption mechanism has been modeled according to the modified Dubinin-Astakhov isotherm model. Initially, the CFD model has been validated on V_1 tank against experimental results available in the literature. Then, simulations have been carried out on V_2 tank to estimate the effect of a storage capacity increase. The simulations on the V_2 tank have been set keeping the same boundary conditions in terms of velocity, density, and temperature at the inlet by doubling the overall amount of hydrogen stored with respect to V_1 tank. The results show corresponding trends in temperature and pressure profiles with only slight differences in their behaviors; in particular, in the final stage of the charging process.

1 Introduction

Decarbonization has been recognized to be an unavoidable strategy to contrast global warming in the next future. In this context, hydrogen can play a crucial role for its physical and chemical properties such as a high Lower Heating Value (LHV=120 MJ/kg), zero CO_2 emissions in the reaction products when oxidized even in fuel cells. However, being H_2 a light gas, it is characterized by a low energy content for unit volume: only 10.7 MJ/Nm^3. Indeed, this low volumetric energy content leads to substantial hurdles for an efficient and economical hydrogen storage, complicating the development of a hydrogen-based economy. Capurso et al. [1], Ge et al. [2] and Widera [3] in their works explain in detail the role of hydrogen in reaching the carbon neutrality goals and its implementation in Renewable Energy Source (RES) based systems by considering both advantages and disadvantages of

hydrogen usage. The increase of hydrogen technology systems is related to the need to increase RES. Being RES not programmable, often there is a mismatch between demand and energy offer; to avoid energy waste, the energy surplus generated by RES can be used for hydrogen production. Then, the development of an efficient hydrogen storage system becomes necessary. The hydrogen low volumetric energy density turns out to be the main issue for hydrogen storage. Currently, hydrogen can be stored in gaseous, liquefied, or in solid state. Usman [4] and Zhou [5], reviewed the currently available hydrogen storage methods and described the advantages and disadvantages for each method. These papers highlight that the hydrogen storage in solid state may be a new way toward efficient storage compared to other conventional methods such as compressed gas and cryogenic liquid. Hydrogen storage in solid state can occur through the use of porous media, where hydrogen is bound through physisorption to materials like activated carbons, Metal Organic Frameworks (MOFs), Covalent Organic Framework (COFs), called adsorbent materials, or by using metal hydrides to store hydrogen through chemisorption. Hydrogen physisorption is considered a promising storage method for storing hydrogen at pressure below 100 bar, and at higher temperatures than those required for liquid storage. In physisorption an attractive interaction born between hydrogen molecules and porous media surfaces due to the Van der Waals forces that do not change the porous structure. Furthermore, compared to chemical storage in metal hydrides, physisorption allows rapid adsorption/desorption kinetics with low heat generated/absorbed. Hermosilla-Lara et al. [6], carried out experimental activities on activated carbon packed bed storage tank. Several tests were carried out in order to investigate the effect of the initial flow rate on the temperature field in the reservoir and on the duration of the charging process. They also studied the contribution of thermal effects to the adsorption mechanism. According to these experimental tests, Xiao et al. [7, 8] validated their numerical model through Computational Fluid Dynamics (CFD). In addition they investigated on the heat supplied/released by the adsorption mechanism during charging, dormancy and discharging processes on axi-symmetric geometry at ambient temperature (295 K) and medium storage pressure (10 MPa). In their work the isotherm adsorption model of Dubinin-Astakhov (D-A) is applied, which is the most widely used model, based on Polanyi's potential theory [9]. Wang et al. [10] proposed a guiding methodology for the selection of adsorption model. Furthermore, other works proposed numerical studies in different room conditions by using the Dubinin-Astakhov model. For instance, Petiptas et al. [11] presented a comparative analysis of the cryo-compression and cryo-adsorption approaches to hydrogen storage, examining their respective storage densities and dormancies as a function of temperature, pressure and type of adsorption material. Xiao et al. [12], investigated on the thermal effects and mass of hydrogen in adsorbed phase at cryogenic temperature, where hydrogen storage tank was cooled by liquid nitrogen (LN_2).
In this work a CFD model for physisorption has been initially validated against experimental [6] and numerical [8] results in the literature [6]; then, the influence of the variation of the tank capacity on the charging, dormancy, and discharging process is investigated.

2 Geometry and Mesh model

The test case, chosen for validation, refers to the work of Xiao et al. [8]. Figure 1 shows the computational domain and Figure 2 shows the mesh. The hydrogen storage system is made of steel, activated carbon is chosen as the material for the porous matrix. Table 1 shows the main geometric parameters of the tank, named V_1. Table 2 shows the properties of hydrogen, activated carbon and steel, respectively. The porous matrix fills the tank with the exception of the inlet pipe. The mesh discretization has been carried out in ANSYS Modeler; V_1 is subdivided in 6493 cells and 7252 nodes, while V_2 geometry is subdivided in 10404 cells and 11348 nodes, preserving the mesh size.

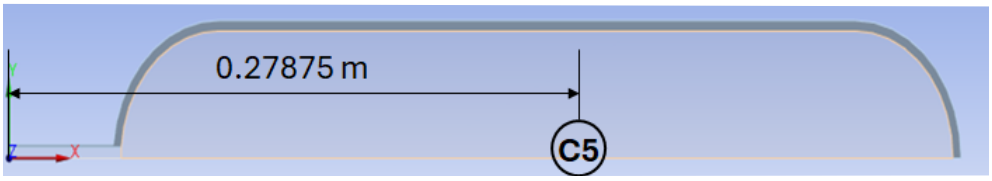

Figure 1: Geometry of the tank V_1.

3 Mathemathical model

CFD simulations have been carried out by means of ANSYS Fluent according to the Reynolds Average Navier-Stokes (RANS) approach in order to simulate the adsorption/desorption mechanism in the porous matrix. The hydrogen is considered as an ideal gas.

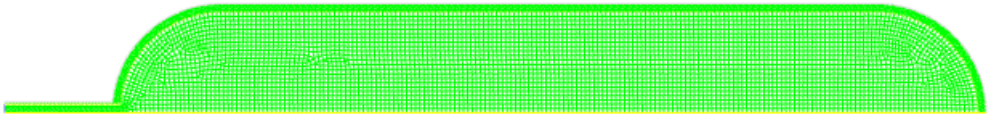

Figure 2: Mesh used for the tank V_1.

Table 1: Geometry parameters for the tank V_1.

Parameter	**Value**
Inner radius (pipe)	4 [mm]
Length (pipe)	53.75 [mm]
Wall Thickness (pipe)	1 [mm]
Length (tank)	400 [mm]
Inner radius (tank)	46.9 [mm]
Thickness (tank)	3.9 [mm]

3.1 Adsorption Isotherm Model

The Modified Dubinin-Astakhov model [13] is used to describe the adsorption/desorption process under supercritical conditions. Activated carbon is chosen as porous material. The number of adsorbed moles of hydrogen per unit of mass of porous matrix, n^* [mol kg^{-1}], in equilibrium with the gas phase, is expressed by:

$$n^* = n_{max} \exp\left[-\left(\frac{RT}{\alpha+\beta T}\right)^m \ln^m\left(\frac{p_o}{p}\right)\right] \tag{1}$$

where n_{max} is the limiting adsorption value equal to 71.6 [mol kg^{-1}], R [J K^{-1} mol^{-1}] is the universal gas constant, p_o is the saturation pressure equal to 1470 [MPa], m is equal to 2 for activated carbon, α is the enthalpic factor equal to 3180 [J mol^{-1}] and β is the entropic factor equal to 18.9 [J K^{-1} mol^{-1}].

3.2 Continuity equation

The mass conservation equation in porous media can be expressed as follows:

$$\frac{(\partial \epsilon_b \rho_g)}{\partial t} + \nabla \cdot (\rho_g \vec{v}) = S_m \tag{2}$$

where ϵ_b is the porosity of the porous matrix and ρ_g [kg/m^3] is the density of hydrogen gas phase. S_m [kg m^{-3} s^{-1}] represents the mass source term which takes into account the amount of adsorbed hydrogen in porous matrix and it is calculated by Eq. 3:

$$S_m = -(1-\epsilon_b)\rho_p M_{H_2} \frac{\partial n}{\partial t} \tag{3}$$

where ρ_p is the apparent density of the porous material equal to 517.6 [kg/m^3], M_{H_2} [kg mol^{-1}] is the molecular weight of hydrogen, $\partial n/\partial t$ is the kinematic adsorption, and n is the number of hydrogen moles actually adsorbed on the porous matrix. The kinematic adsorption can be computed as follows:

$$\frac{\partial n}{\partial t} = k(n^* - n) \tag{4}$$

where k is the mass transfer coefficient equal to 0.15 [s^{-1}]. Equation (4) was fitted using the linear driving force model (LDF) [14], which is one of the most widely used methods to describe the dynamic of adsorption in fixed-bed adsorbers.

Table 2: Material Properties

Description	Properties	Value
Hydrogen	Density [kg/m^3]	Ideal Gas
	Specific Heat Capacity [J/(kg m^3)]	14700
	Thermal conductivity [W/(m K)]	0.206
	Viscosity [Pa s]	8.411e-6
	Viscous Resistance coefficient [m^{-2}]	8.29055e7
	Inertial Resistance coefficient [m^{-1}]	7586
Activated Carbon	Porosity	0.49
	Apparent Density [kg/m^3]	517.6
	Specific Heat Capacity [J/(kg m^3)]	825
	Thermal conductivity [W/(m K)]	0.646
Steel	Density [kg/m^3]	7830
	Specific Heat Capacity [J/(kg m^3)]	468
	Thermal conductivity [W/(m K)]	13

3.3 Momentum equation

The momentum equation in the porous matrix is the following:

$$\frac{\partial}{\partial t}(\rho_g \overrightarrow{v}) + \nabla \cdot (\rho_g \overrightarrow{v}\,\overrightarrow{v}) = -\nabla p + \nabla \cdot \bar{\bar{\tau}} + \rho_g \overrightarrow{g} + \overrightarrow{S_f} \tag{5}$$

where $\bar{\bar{\tau}}$ is the stress tensor and $\overrightarrow{S_f}$ is the momentum source term [N m^{-3}] based on the Ergun equation which includes viscous and inertial losses. In each direction i, $\overrightarrow{S_f}$ is expressed as:

$$S_{fi} = -\left(\frac{\mu}{\kappa} v_i + C_2 \frac{1}{2} \rho_g |\overrightarrow{v}| v_i\right) \tag{6}$$

where μ [$Pa\ s$] is the dynamic viscosity of hydrogen gas, $1/\kappa$ [1/m^2] is the viscous resistance coefficient, C_2 [m^{-1}] the internal resistance coefficient, $\overrightarrow{v}$ is the magnitude of the velocity vector and v_i is the velocity component along the $i-th$ direction.

3.4 Energy equation

The energy equation for the hydrogen storage tank expresses the balance between the amount of energy accumulated in the tank and the energy variations due to convection, pressure work, conduction and thermal dispersion fluxes and heat release/absorption due to the adsorption/desorption:

$$\frac{\partial}{\partial t}\left[\epsilon_b \rho_g E_g + (1-\epsilon_b)\rho_p E_s\right] + \nabla \cdot \left[\overrightarrow{v}(\rho_g E_g + p)\right] = \nabla \cdot \left(\kappa_{eff} \nabla T - \sum_i h_i \overrightarrow{J_i} + \bar{\bar{\tau}} \cdot \overrightarrow{v}\right) + S_e \tag{7}$$

The contribution of the hydrogen adsorbed phase is accounted by S_e [J m^{-3} s^{-1}], the energy source term:

$$S_e = \frac{-\Delta H\, S_m}{M_{H_2}} \tag{8}$$

where ΔH [J mol^{-1}] is the isosteric entalpy, which in this case is not constant but changes according to adsorbed/desorbed phase of hydrogen in the tank, as indicated by Eq. 9:

$$\Delta H = \alpha \sqrt{\ln\left(\frac{n^*}{n}\right)} \tag{9}$$

4 Initial and boundary conditions

Table 3 shows the initial condition of hydrogen storage tank. In Table 4 the different boundary conditions of both tanks in terms of mass flow rate during the three phases (charge, dormancy, discharge) are shown. The boundary conditions used for tank V_2 were obtained by holding density and inlet flow velocity constant during charging. Since, the pipe cross section of tank V_2 is increased only by a factor of 1.587 compared with that of tank V_1, in order to store twice hydrogen mass in the tank V_2, the time of charging process was modified from 442 [s] for tank V_1 to 557 [s] for tank V_2. Instead, the discharge time was kept constant between the two cases, as shown in the Table 4. A heat transfer coefficient, H_c, equal to 36 [W/(m^2 K)] has been considered.

Table 3: Initial Condition.

Parameter	**Value**
T_{in}	303 [K]
T_{wall}	302 [K]
T_{amb}	302 [K]
$T_{internal}$	302 [K]
P_{in}	48580 [Pa]

Table 4: Boundary Conditions.

	V$_1$ Tank		**V$_2$ Tank**	
Process	**Time**	**Mass Flow Rate**	**Time**	**Mass Flow Rate**
Charge	0-442 [s]	4.355e-05 [kg/s]	0-557 [s]	6.9131e-05 [kg/s]
Dormancy	442-3046 [s]	0 [kg/s]	557-3046 [s]	0 [kg/s]
Discharge	3046-3097 [s]	-2.186e-05 [kg/s]	3046-3097 [s]	-4.41e-05 [kg/s]

5 Model Validation

The model validation has been carried out by comparison of the simulations results against experimental data presented by Hermosilla-Lara at al. [6]. Figure 3 shows the comparison between experimental and numerical temperature (a) and pressure (b) measurements in point C_5 located on the tank axis at 0.27875 [m] from the inlet section (see figure 1). The numerical result are in good agreement with experimental results. Actually during the charging phase, the temperature rise is faster and a higher max temperature is reached.

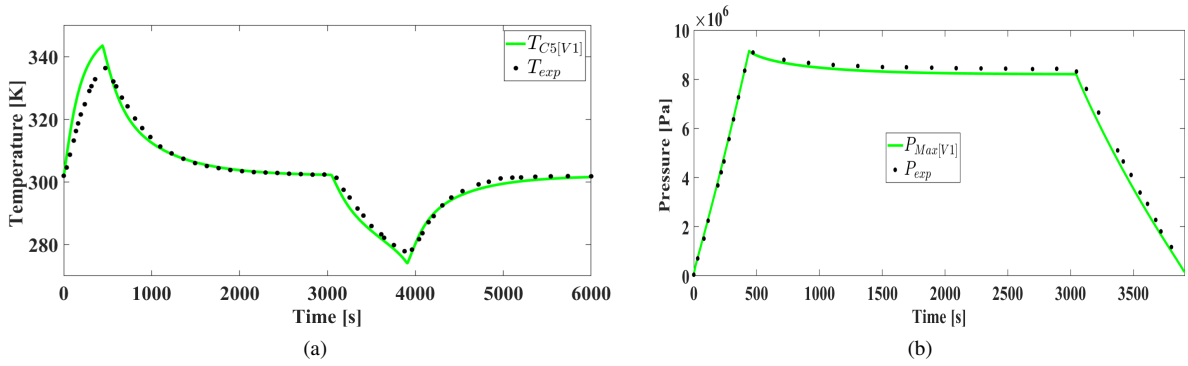

(a) (b)

Figure 3. Comparison with experimental results: (a) Temperature profile in C_5 point , (b) Maximum pressure profile

6 Results and discussion

The goal of this works is to numerically investigate, by means of CFD, the relation between storage capacity and the mass of hydrogen adsorbed by the porous carbon matrix. In particular, a geometrically similar tank has been considered by doubling the volume ($V_2 = 2\ V_1$). The numerical results in terms of pressure, temperature and mass have been compared for the two cases, V_1 and V_2.

6.1 Pressure results

The pressure reaches its maximum value at the end of the charging process in both cases (see Figure 4). During dormancy, the pressure slightly drops due to heat exchange with the environment, lowering the temperature, and hence, the pressure.

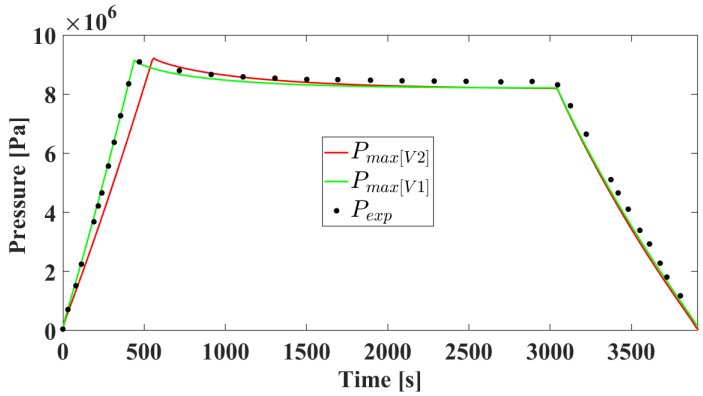

Figure 4: Comparison between experimental and numerical results for tanks V_2 and V_1 in terms of pressure profiles.

6.2 Temperature results

Regarding the monitoring point C_5, the temperature reaches its maximum value at the end of the charging process. This is due to the heat released by adsorption process which is controlled by the isosteric enthalpic factor in Eq. 9. The overall trend of temperature cycle in tank V_2 is similar to that in tank V_1. Figure 5 shows the temperature trends in charging, dormancy and discharging phases of both V_2 and V_1 tanks.

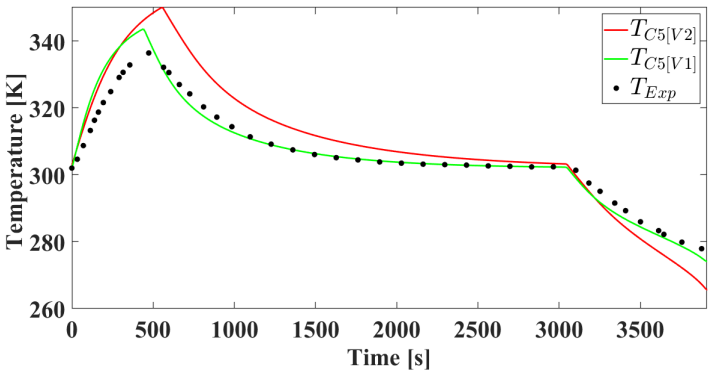

Figure 5: Comparison between Temperature profile in tank V_2, V_1 and experimental results on monitoring point C_5.

In V_2 tank, the temperature reaches a higher value than V_1 tank at the end of charging phase. This is due to a greater amount of hydrogen adsorbed in the porous matrix, hence a greater number of moles involves a greater isosteric enthalpic factor in Eq. 9 and a worse heat exchange with the ambient. During the dormancy phase, V_2 tank exhibits a more intense local heat exchange with the surrounding environment compared to V_1 tank, because the heat transfer turns out to be proportional to the internal exchange surface area. In the discharging phase, in V_2

tank, the temperature drops faster with respect to V_1 tank. The temperature reaches the minimum value at the end of the discharge process in both cases. The difference in the values of the minimum temperatures between the two cases is due to the higher mass flow rate at the outlet of the larger V_2 tank. Keeping the discharge period of time constant, a higher mass flow rate was set at the outlet section of tank V_2 in order to drain twice mass of hydrogen with respect with in tank V_1. Temperature contours referring to V_2 tank are shown in Figure 6. Through these contours it is possible to identify the zone, inside the tank, where the maximum and minimum temperature peaks are reached in the charging and discharging phase, respectively. A temperature gradient from the outer wall to the axis of the tank is observed in both the charging and discharging phases.

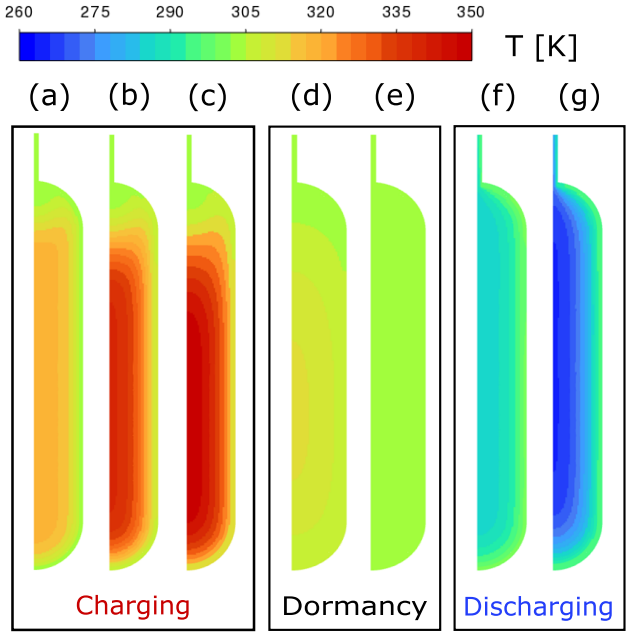

Figure 6: Temperature contour of V_2 tank at: (a) 100 *s*, (b) 300 *s*, (c) 557 *s*, (d) 1500 *s*, (e) 3046 *s*, (f) 3400 *s*, (g) 3907 *s*.

6.3 Mass Analysis

In V_2 tank, the total amount of hydrogen mass (0.0384 kg) is actually doubled with respect to V_1 as reported in table 4. In Figure 7 the evolution of hydrogen transition from gas to adsorbed phase is shown for V_2 tank. The adsorbed hydrogen slightly increase during the dormancy process until saturation of the porous matrix. The increase of adsorbed phase in the tank is also due to the temperature decrease during dormancy due to heat exchange according to the Dubinin-Astachov model. The sum of adsorbed and gaseous phase follows the total mass introduced in the tank at the end of the charging, as shown in Figure 7. In Figure 8, the mass profiles in both cases are compared.

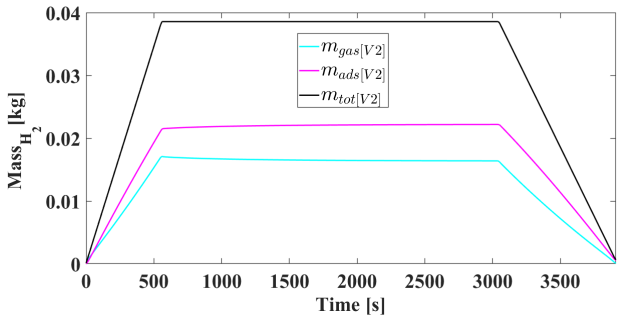

Figure 7: Profile of hydrogen mass in gas and adsorbed phase in overall cycle in V_2 tank.

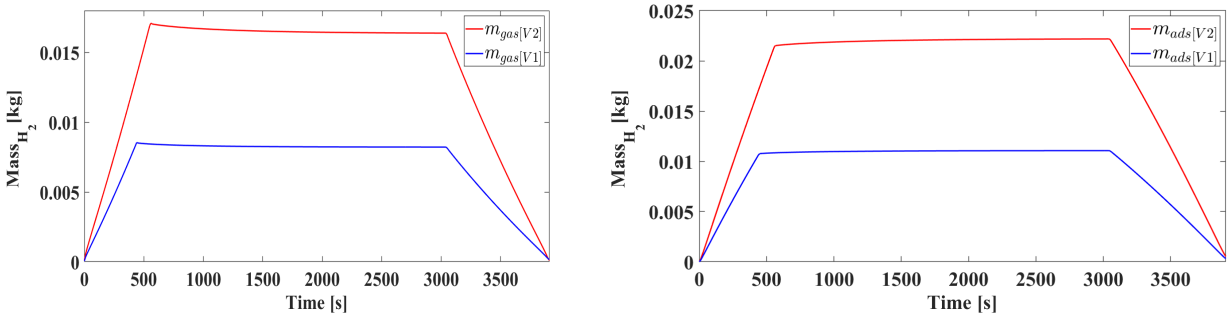

Figure 8. Comparison between Mass profile in V_1 and V_2 geometry: (a) Mass in gaseous phase (b) Mass in adsorbed phase

7 Conclusions

A numerical analysis has been carried out to investigate the effect of geometry scaling on the thermal behavior inside a hydrogen storage tank. The adsorption and desorption processes have been modeled with the modified Dubinin-Astakhov model in ANSYS Fluent through user defined functions. In this work, isosteric entalpy plays an important role in order to reach the temperature peak at the end of charging phase in V_2 tank. It has been shown how doubling the tank volume the heat exchange with the surrounding environment worsen. The adsorbed hydrogen mass has been investigated in V_2 tank, in comparison with V_1 tank. It was also verified that increasing the size of the tank results in a maximum pressure level inside the tank, which remains almost unchanged. This allows us to say that, at least at these sizes, the scaled-up system for stationary hydrogen storage applications can be used.

Acknowledgments

This work was partly supported by the Italian Ministry of University and Research under the Programme "Department of Excellence" Legge 232/2016 (Grant No. CUP - D93C23000100001) and supported under the National Recovery and Resilience Plan (NRRP), Measurement M2C2 Investment 3.5 - Call for "Ricerca e sviluppo sull'idrogeno"- Project code: RSH2A_000035 "Novel Materials for Hydrogen storage" - CUP: F27G22000180006.

References

[1] T. Capurso, M. Stefanizzi, M. Torresi, and S. Camporeale, "Perspective of the role of hydrogen in the 21st century energy transition," *Energy Conversion and Management*, vol. 251, p. 114898, 2022.

[2] L. Ge, B. Zhang, W. Huang, Y. Li, L. Hou, J. Xiao, Z. Mao, and X. Li, "A review of hydrogen generation, storage, and applications in power system," *Journal of Energy Storage*, vol. 75, p. 109307, 2024.

[3] B. Widera, "Renewable hydrogen implementations for combined energy storage, transportation and stationary applications," *Thermal Science and Engineering Progress*, vol. 16, p. 100460, 2020.

[4] M. R. Usman, "Hydrogen storage methods: Review and current status," *Renewable and Sustainable Energy Reviews*, vol. 167, p. 112743, 2022.

[5] L. Zhou, "Progress and problems in hydrogen storage methods," *Renewable and Sustainable Energy Reviews*, vol. 9, no. 4, pp. 395–408, 2005.

[6] G. Hermosilla-Lara, G. Momen, P. Marty, B. Le Neindre, and K. Hassouni, "Hydrogen storage by adsorption on activated carbon: investigation of the thermal effects during the charging process," *International journal of hydrogen energy*, vol. 32, no. 10-11, pp. 1542–1553, 2007.

[7] J. Xiao, L. Tong, C. Deng, P. Bénard, and R. Chahine, "Simulation of heat and mass transfer in activated carbon tank for hydrogen storage," *International journal of hydrogen energy*, vol. 35, no. 15, pp. 8106–8116, 2010.

[8] J. Xiao, R. Peng, D. Cossement, P. Bénard, and R. Chahine, "Cfd model for charge and discharge cycle of adsorptive hydrogen storage on activated carbon," *International journal of hydrogen energy*, vol. 38, no. 3, pp. 1450–1459, 2013.

[9] C. T. Chiou, *Partition and adsorption of organic contaminants in environmental systems*. John Wiley & Sons, 2003.

[10] J. Wang and X. Guo, "Adsorption isotherm models: Classification, physical meaning, application and solving method," *Chemosphere*, vol. 258, p. 127279, 2020.

[11] G. Petitpas, P. Bénard, L. E. Klebanoff, J. Xiao, and S. Aceves, "A comparative analysis of the cryo-compression and cryo-adsorption hydrogen storage methods," *International journal of hydrogen energy*, vol. 39, no. 20, pp. 10564–10584, 2014.

[12] J. Xiao, L. Tong, D. Cossement, P. Bénard, and R. Chahine, "Cfd simulation for charge–discharge cycle of cryo-adsorptive hydrogen storage on activated carbon," *International Journal of Hydrogen Energy*, vol. 37, no. 17, pp. 12893–12904, 2012.

[13] M.-A. Richard, P. Bénard, and R. Chahine, "Gas adsorption process in activated carbon over a wide temperature range above the critical point. part 1: modified dubinin-astakhov model," *Adsorption*, vol. 15, pp. 43–51, 2009.

[14] H. Naidu and A. P. Mathews, "Linear driving force analysis of adsorption dynamics in stratified fixed-bed adsorbers," *Separation and Purification Technology*, vol. 257, p. 117955, 2021.